

PHOTOPROTONS FROM Nb⁹³

R. M. OSOKINA

P. N. Lebedev Physics Institute, Academy of Sciences, U.S.S.R.

Submitted to JETP editor August 2, 1962

J. Exptl. Theoret. Phys. (U.S.S.R.) 44, 444-453 (February, 1963)

The angular and energy distributions and the yield of photoprotons from Nb⁹³ are measured by the nuclear emulsion technique for three peak bremsstrahlung energies $E_{\gamma \max} = 19.5, 23.5, \text{ and } 27.5$ MeV. The results are compared with the statistical theory of nuclear reactions, with the effect of nucleon pair correlations on the level density of the residual nucleus taken into account. It is shown that the measured photoproton yield exceeds the theoretical yield by an order of magnitude. The photoproton spectrum is much harder than the evaporation spectrum. The angular distributions exhibit anisotropy of the form $I(\theta) = a + b \sin^2 \theta$. From an analysis of the angular distributions it is concluded that the $2p \rightarrow 2d$ E1 proton transitions play an important part.

INTRODUCTION

IT can be regarded as established that the level densities of even-Z and even-N nuclei have a gap at the ground level due to pair correlations. The size Δ of the gap is the sum of the proton and neutron pairing energies: $\Delta = \delta_p + \delta_n$. However, in the analysis of photonuclear reactions pair correlations have hitherto not been taken into account. Also, it follows from a comparison of the experimental photoproton yields with the statistical theory that for medium-weight nuclei having a proton binding energy B_p smaller than the neutron binding energy B_n the observed yields can be accounted for by the evaporation model. [1-4] Nevertheless, data regarding angular and energy distributions and the dependence of the photoproton yield on $E_{\gamma \max}$ are not always consistent with the statistical theory. [5-7]

Pair correlations are taken into account in actual practice by calculating the nuclear excitation energy from some "characteristic" level lying above the ground state by the amount Δ of the gap: $E^* - E' = E^* - \Delta$; the level density of the final nucleus then becomes $\omega(E')$ instead of $\omega(E^*)$. This results in a large change of the probability ratio of proton and neutron evaporation compared with the calculations performed neglecting pair correlations for final nuclei of different evenness-oddness type. Thus when odd-even nuclei are excited by γ quanta the emission of a proton results in an even-even nucleus with $\Delta = \delta_p + \delta_n$, while neutron emission results in an odd-odd nucleus with $\Delta = 0$. The existence of an energy gap in the

first of these nuclei leads to considerably increased competition of the (γ, n) reaction and therefore to a reduced yield of evaporated photoprotons. The opposite tendency is observed in even-odd nuclei; the yield of evaporated photoprotons increases considerably when pair correlations are taken into account. For even-even initial nuclei the calculation will be practically independent of the correlation, since both final nuclei possess an energy gap of the same extent. It can thus be expected that the photoproton yield from odd-even nuclei will result to a considerable degree from a non-evaporation mechanism, even if the proton binding energy B_p is smaller than the neutron binding energy B_n and the barrier is relatively low. One such nucleus is Nb⁹³, which can be analyzed in a simple manner because niobium is anisotropic.

MEASURING TECHNIQUE

The measuring technique and apparatus were described in detail in [6,7]. However, the design of the inner movable part of the chamber containing the target and plates was modified considerably. First, the amount of matter in the immediate vicinity of the beam was considerably reduced; the duraluminum previously used for the inside walls and plate and target holders was replaced by polystyrene (CH₂)_n and graphite. The (γ, p) threshold of carbon is quite high ($B_p = 16$ MeV for C¹² and 16.2 MeV for C¹³); the proton background was thus made several times smaller. Second, steps were taken to reduce the uncontrollable errors in solid

angles resulting from inaccurate adjustments of the plate holders and of the beam center at the target. For this purpose, when measuring angular distributions, instead of several plates placed around the target at different angles θ with respect to the γ beam, two plates positioned symmetrically about the beam were used. These plates covered the intervals $\theta = 10-120^\circ$ and $60-170^\circ$, respectively. The 2×6 cm target was suspended by Kapron fibers at 20° to the γ beam so as to be fully within the beam. Figure 1 shows the arrangement of the target and photographic plates.

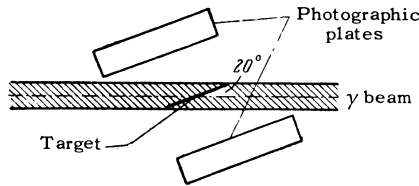


FIG. 1. Arrangement of target and photographic plates.

The target was a foil of chemically pure niobium 27.7 mg/cm^2 thick. Protons were registered in NIKFI-T3 emulsions 300μ thick. The emulsions were scanned with MBI-2 binocular microscopes having an $\times 60$ objective and $\times 5$ eyepiece; tracks were measured with an $\times 7$ eyepiece. The standard MBI-2 microscope stage was replaced with another stage permitting the scanning of large areas. Proton energies were obtained from the range-energy curve for Ilford C-2 emulsions,^[8] with a correction for the density difference of the Ilford C-2 and NIKFI-T3 emulsions. The total proton range was the sum of the range in the target and the residual range in the emulsion. The range in the target was taken to be the effective target half-thickness converted from known relations between ionization losses and ranges in emulsion.

An Ural computer was used in treating the experimental data, beginning with track selection according to direction and ending with assignments to angular and energy intervals. The proton background resulting from scattered γ rays was found to be 1–2% in irradiation of a targetless chamber.

RESULTS

Irradiation was performed at the 30-MeV synchrotron of the Physics Institute of the USSR Academy of Sciences with three values of $E_{\gamma \text{ max}}$: 19.5, 23.5, and 27.5 MeV. Table I gives the following data for each run: M—the dose in monitor counts reduced to identical ionization in a thick-walled ionization chamber, S—the combined areas meas-

Table I

$E_{\gamma \text{ max}}$, MeV	M	S, cm ²	N_p	n_b
19.5	12330	16	2221	13
23.5	7060	16	2605	30
27.5	10400	8	2937	36

ured on the two plates, N_p —the total number of proton tracks with $\epsilon_p \geq 3.0$ MeV beginning at the surface and satisfying the geometric selection criteria with a background correction, and n_b —the number of background tracks relative to the dose M and scanned area.

Figure 2 shows the photoproton energy distributions in relative units. $F(\epsilon_p)$ is the ratio of the number of protons having energies in the interval $\Delta\epsilon_p = 0.5$ MeV to the total number N_p of protons.

Figure 3 shows the angular distributions of

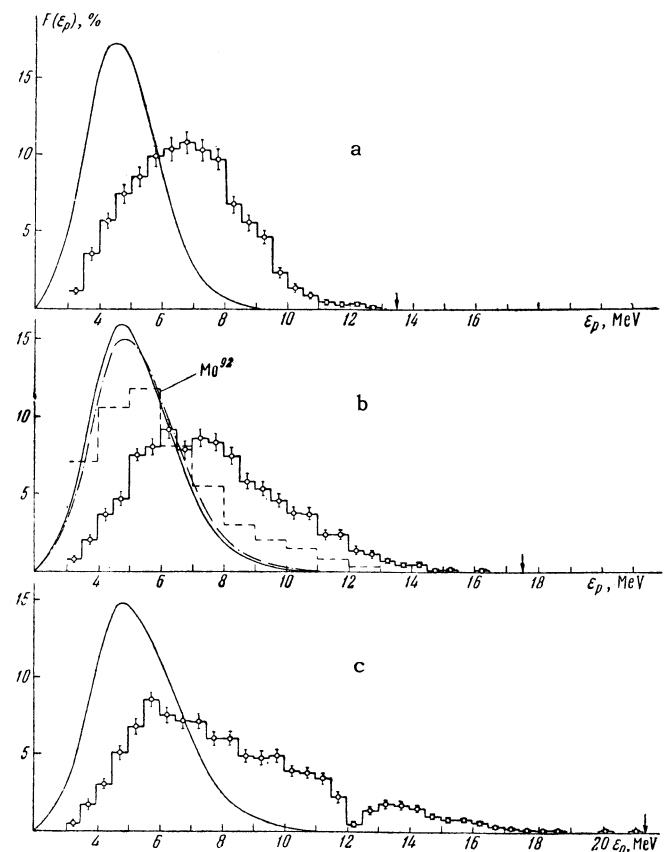


FIG. 2. Energy distributions of photoprotons from Nb^{93} for $E_{\gamma \text{ max}} = 19.5$ MeV (a), 23.5 MeV (b), and 27.5 MeV (c). The histograms are the experimental spectra. The dashed histogram in Fig. 2b is the photoproton spectrum of Mo^{92} .^[3] The smooth curves are spectra computed from the evaporation model for level density ω_1 taking account of pair correlations. The dashed curve in Fig. 2b is the same, neglecting pair correlations. Arrows indicate the maximum possible proton energy $\epsilon_{p \text{ max}} = E_{\gamma \text{ max}} - B_p$.

FIG. 3. Angular distributions of photoprotons from Nb⁹³ for E_{γmax} = 19.5 MeV (a), 23.5 MeV (b), and 27.5 MeV (c). The histograms are the experimental results. The smooth curves represent distributions of the forms I(θ) = a + b sin² θ and I(θ) = a + b sin² θ + c sin² θ cos θ. The parameters a, b, and c obtained by least squares are given in Table II.

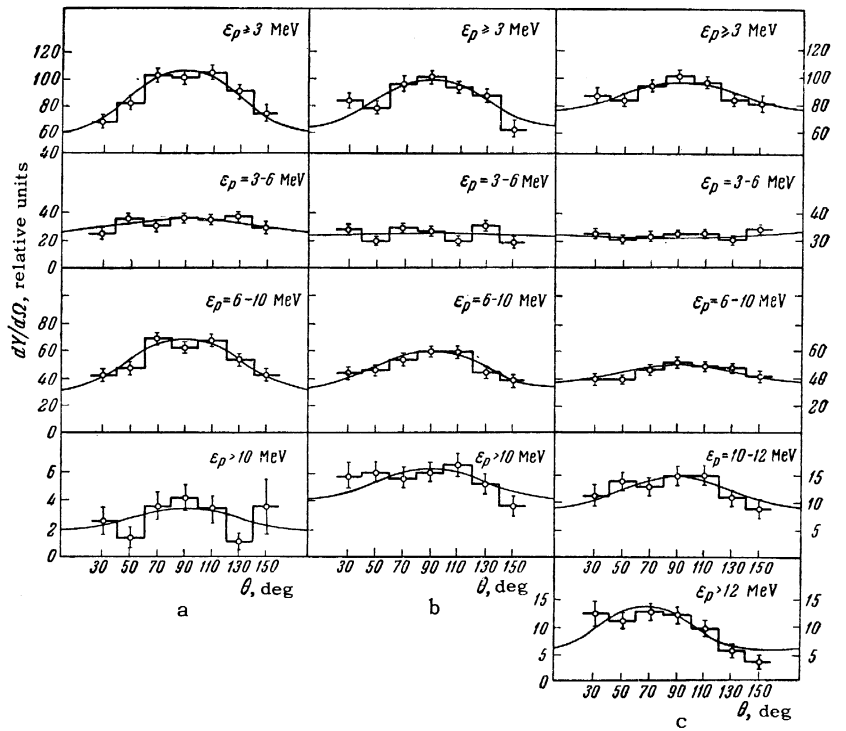


Table II. Angular distribution parameters obtained by least squares

E _{γmax} , MeV	19,5			23,5			27,5				
	a	b	b/a	a	b	b/a	a	b	c	b/a	c/a
All protons	60,0±5,1	45,1±7,3	0,75±0,18	63,7±4,7	34,4±6,5	0,54±0,15	75,1±5,3	21,3±6,8	—	0,28±0,11	—
≥3 MeV	—	—	—	—	—	—	—	—	—	—	—
3-6 MeV	26,5±3,2	8,5±4,4	0,32±0,20	22,1±2,8	3,0±2,7	0,14±0,13	25,4±2,8	-3,1±3,8	—	-0,12±0,14	—
6-10 MeV	29,9±3,9	37,3±5,6	1,25±0,34	31,1±3,3	26,2±4,9	0,84±0,25	35,5±3,2	12,8±4,5	—	0,36±0,17	—
>10 MeV	3,6±1,3	-0,7±1,7	-0,19±0,53	10,5±1,8	5,2±2,5	0,49±0,33	14,3±2,2	11,6±3,2	10,6±3,1	0,81±0,34	0,74±0,22
10-12 MeV	—	—	—	—	—	—	8,4±1,6	6,1±2,2	2,2±2,1	0,72±0,39	0,26±0,29
>12 MeV	—	—	—	—	—	—	5,9±1,5	5,6±2,1	7,8±1,9	0,94±0,58	1,31±0,39

protons in different energy groups. Ordinates represent the proton yield (in the angular interval Δθ = 20°) emitted at the angle θ to the γ-beam direction. For all three values of E_{γmax} the proton yield with ε_p ≥ 3 MeV for Δθ = 80–100° was taken as 100. The angular distributions were approximated by curves of the form

$$I(\theta) = a + b \sin^2 \theta.$$

An exception was found in the distribution of fast protons (ε_p > 10 MeV) for E_{γmax} = 27.5 MeV, which exhibited considerable asymmetry about 90°. This distribution was approximated by

$$I(\theta) = a + b \sin^2 \theta + c \sin^2 \theta \cos \theta.$$

The parameters a, b, and c obtained by least squares are given in Table II, as well as the ratios b/a characterizing the anisotropy of the angular distributions.

It is easily shown that for a reaction yielding an angular distribution represented by I(θ) = a + b sin² θ the integral yield is

$$Y = \int_0^{2\pi} I(\theta) \sin^2 \theta d\theta = K \left(a + \frac{4}{3} b \right),$$

where K is a factor depending on the normalization of a and b.

The relative integral yields of protons with $\epsilon_p \geq 3$ MeV for $E_{\gamma \max} = 19.5, 23.5,$ and 27.5 MeV were $1.00 \pm 0.04, 1.58 \pm 0.04,$ and $2.22 \pm 0.10,$ respectively. The absolute integral yields were obtained by a comparison with the previously measured photoproton yield of a sample enriched in Cu^{65} .^[7] Figure 4 shows the photoproton yields from Nb^{93} obtained in the present work, compared with results given by other authors^[9,4] and the dependence of the neutron yield on $E_{\gamma \max}$, measured in^[10-12] by direct registration of neutrons.

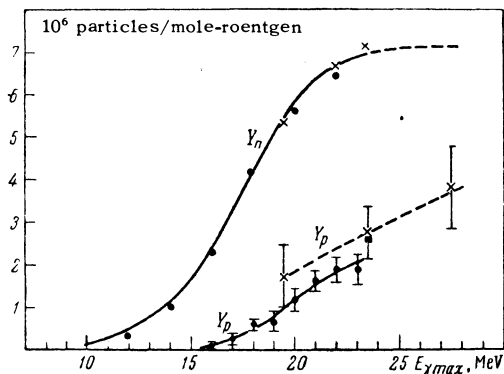


FIG. 4. Dependence of photoproton yield Y_p and photo-neutron yield Y_n from Nb^{93} on $E_{\gamma \max}$. For Y_p : \times —present work, \bullet —^[9], \blacksquare —^[4]; the yields have been multiplied by the factor 5. For Y_n : \times and \bullet —measured in ^[11] and ^[12], respectively; the smooth curve was obtained in ^[10].

DISCUSSION OF RESULTS

The results were analyzed to determine the relative contributions of evaporation and the direct photoeffect to the photoproton yield from niobium. For this purpose the experimental yield ratio Y_p/Y_n (Fig. 4) was compared with the calculated ratio based on the statistical theory.

If the cross section $\sigma_{\gamma n}(E)$ is known the statistical theory gives the photoproton yield obtained from the bremsstrahlung spectrum $N(E_\gamma, E_{\gamma \max})$:

$$Y_p(E_{\gamma \max}) = \int_0^{E_{\gamma \max}} \sigma_{\gamma n}(E_\gamma) N(E_\gamma, E_{\gamma \max}) \eta(E_\gamma) dE_\gamma,$$

where $\eta(E_\gamma)$ is the ratio of the total proton width to the total neutron width.

The calculation was performed for the two most frequently used dependences of the residual-nucleus level density on its excitation energy E^* : $\omega_1 \sim \exp[2(aE^*)^{1/2}]$, where A is the atomic weight and a was taken as $A/10$,^[13] and $\omega_2 \sim \exp(E^*/T)$, where $T = 1$ MeV is the nuclear temperature; $E^* = \epsilon_{\max} - \epsilon$, where ϵ_{\max} is the maximum possible energy of an emitted particle and equals $E_\gamma - B$ or $E_\gamma - (B + \Delta)$ depending, respectively, on whether pair correlations are neglected or taken into account.

The reaction thresholds B and the evaporation energies $\Delta = \delta_p + \delta_n$ are given in Table III. The cross section $\sigma_n(\epsilon_n)$ was taken from the book of Blatt and Weisskopf;^[18] $\sigma_p(\epsilon_p)$ was taken from tables in ^[19]; r_0 was taken to be 1.65×10^{-13} cm following Evans,^[20] who showed that the Coulomb barrier of a nucleus having a diffuse boundary (for a charge distribution obtained from electron scattering experiments) can be approximated by the barrier for a nucleus with uniform density assuming $r_0 = 1.65 F$.

Figure 5 shows the measured and calculated dependences of the photoproton-to-photoneutron yield ratio on $E_{\gamma \max}$. It should be noted that somewhat different quantities are compared in the experimental and theoretical calculations. Thus the theory compares the yields of reactions in which a proton or neutron is the primary emitted particle:

Table III. Photonuclear reaction thresholds for Nb^{93} and total evaporation energies $\Delta = \delta_p + \delta_n$ in final nuclei

Reaction	Threshold B, MeV	Final nucleus		δ_p , MeV	δ_n , MeV	Δ	$B + \Delta$
		Z	N				
(γ, n)	$8.82 \pm 0.05^*$	51	41	—	—	—	8.82
(γ, p)	$5.94 \pm 0.1^{**}$	52	40	0.92****	1.31****	2.23	8.15
(γ, np)	14.84***	51	40	—	1.31****	1.31	16.17
(γ, pn)	15.46***	52	39	0.92****	—	0.92	16.38
$(\gamma, 2p)$	16.89***	50	41	1.84****	—	1.84	18.73

*Average of values of B_n given in ^[14].

**Obtained from β -decay data using the formula $B_n - B_p = Q_{EC} = 0.783$, where $Q_{EC} = 2.1$ MeV was taken from tables in ^[15].

***Calculated from the mass formula.^[16]

****See ^[17].

$$Y_p^{\text{theor}} = Y_{p_1} = Y_{p_1,\gamma} + Y_{p_1,n} + Y_{p_1,p},$$

$$Y_n^{\text{theor}} = Y_{n_1} = Y_{n_1,\gamma} + Y_{n_1,n} + Y_{n_1,p}.$$

On the other hand, the yields measured by direct registration contain secondary particles:

$$Y_p^{\text{exp}} = Y_{p_1} + Y_{n,p_2} + Y_{p,p_2},$$

$$Y_n^{\text{exp}} = Y_{n_1} + Y_{n,n_2} + Y_{n,p_2}.$$

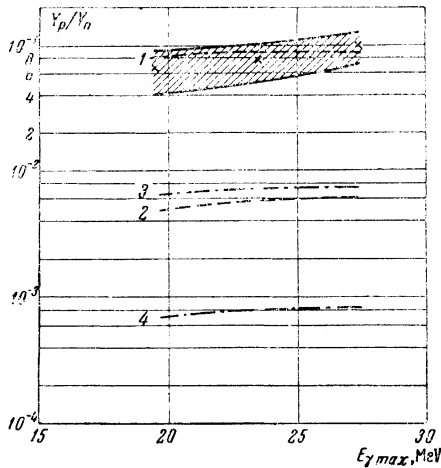


FIG. 5. The photoproton-to-photoneutron yield ratio from Nb⁹³ as a function of $E_{\gamma \text{max}}$. Crosses designate the experimental ratios; the shaded area is that bounded by experimental errors. The dashed lines represent the evaporation-model calculations using different hypotheses regarding the dependence of the final-nucleus level density on the excitation energy: Curve 1— $\omega(E^*) = \exp[2(aE^*)^{1/2}]$, curve 2— $\omega(E^*) = \exp\{2[a(E^* - \Delta)]^{1/2}\}$, curve 3— $\omega(E^*) = \exp(E^*/T)$; curve 4— $\omega(E^*) = \exp[(E^* - \Delta)/T]$.

The secondary-reaction thresholds given in Table III show that these reactions play some part even for $E_{\gamma \text{max}} = 19.5$ MeV. For the purpose of bringing the theory into accord with experiment, one could calculate the contribution of secondary particles on the statistical theory and introduce a suitable correction of Y_p^{theor} and Y_n^{theor} . However, this would require a laborious triple numerical integration. We therefore attempted to calculate roughly the contribution of secondary particles to experimental yields based on the relative yield from the reaction Nb⁹³($\gamma, 2n$)Nb⁹¹,^[12] assuming that the proton/neutron yield ratio from the residual nuclei following (γ, n) and (γ, p) reactions is the same as for Nb⁹³. When the theoretical yield ratio Y_p/Y_n was compared with the experimental ratio uncorrected for the contribution of secondary processes the error was found to be at most a few percent.

Figure 5 shows that the theoretical values of Y_p/Y_n for a level density of the form $\omega_1 = \exp[2(aE^*)^{1/2}]$ neglecting pair correlations agree with experiment. Allowance for pair correlations reduces the theoretical value by more than one order of magnitude. In the case of a level density at constant temperature the theoretical proton yield is considerably smaller than the experimental value both with and without taking account of the evaporation energy. The agreement of the experimental proton/neutron yield ratio with the theoretical ratio based on the level density ω_1 neglecting pair correlations is most probably accidental. Indeed, a comparison of the experimental energy distributions with those calculated on the evaporation model shows that for all the values of $E_{\gamma \text{max}}$ these distributions differ considerably (Fig. 2). Figure 2b also shows that the shape of the evaporation spectrum is almost independent of pair correlations.

It is interesting to compare the results with the (γ, p) reaction in a neighboring even-even isotope Mo⁹² in which, as in Nb⁹³, the proton binding energy is small. However, the evenness-oddness type of nuclei remaining following (γ, p) and (γ, n) reactions in Mo⁹² is such that allowance for pair correlations does not reduce the proton evaporation probability, and it can be expected that the (γ, p) reaction in Mo⁹² will be described by the evaporation model. Indeed, it has been found in^[3] that for $E_{\gamma \text{max}} = 22$ MeV the photoproton yield from Mo⁹², comprising almost 50% of the neutron yield, and the energy distribution are accounted for by the evaporation model. The photoproton spectrum from Mo⁹², shown for comparison in Fig. 2b, is considerably softer than the photoproton spectrum from Nb⁹³ and agrees essentially with the statistical theory; a discrepancy occurs only at high proton energies.

The angular distributions of the photoprotons from Nb⁹³ exhibit considerable anisotropy; this furnishes additional proof that the (γ, p) reaction in this isotope involves a mechanism different from evaporation. It follows from the symmetry of angular distributions about 90° that photoprotons are emitted as a result of the dipole absorption of γ quanta. Some admixture of quadrupole absorption is found only in the case of protons with $\epsilon_p > 10$ MeV for $E_{\gamma \text{max}} = 27.5$ MeV, where the peak is shifted forward. Table IV gives the E1 proton transitions of Nb⁹³ and the anisotropy of the photoproton angular distributions in these transitions calculated in accordance with^[21]. By comparing the theoretical values of b/a in Tables IV

Table IV. E1 proton transitions in Nb⁹³ and anisotropy of photoproton angular distributions in these transitions

Transition	Transition strength [22]	Ratio b/a [21]	Transition	Transition strength [22]	Ratio b/a [21]
$2p_{1/2} \rightarrow 2d_{3/2}$	0.186	1.5	$2p_{3/2} \rightarrow 2d_{7/2}$	0.037	1.5
$1f_{5/2} \rightarrow 1g_{7/2}$	0.837	0.83	$1f_{7/2} \rightarrow 1g_{9/2}$	1.09	0.83
$1f_{3/2} \rightarrow 2d_{5/2}$	0.060	0.083	$1f_{7/2} \rightarrow 2d_{5/2}$	0.085	0.083
$2p_{3/2} \rightarrow 2d_{5/2}$	0.366	1.5	$1f_{7/2} \rightarrow 1g_{7/2}$	0.031	0.83
$2p_{1/2} \rightarrow 3s_{1/2}$	0.080	0			

with the experimental values (Table II) we can conclude that protons having energy $\epsilon_p = 6-10$ MeV for $E_{\gamma \max} = 19.5$ MeV ($b/a = 1.25 \pm 0.34$) result from a $2p \rightarrow 2d$ transition for which $(b/a)_{\text{theor}} = 1.5$, the transition energy being under 19 MeV. The reduced proton anisotropy in the given ϵ_p interval for increased $E_{\gamma \max}$ is evidently associated with the fact that $l \rightarrow l-1$ transitions begin to play a part, producing a practically isotropic distribution. The isotropic distribution of slow protons ($\epsilon_p = 3-6$ MeV) is possibly associated with the fact that in this energy region evaporated protons make a large contribution. However, it is also possible that these protons result from a $2p \rightarrow 3s$ transition, for which $(b/a)_{\text{theor}} = 0$. An intense proton group with $\epsilon_p > 10$ MeV observed for $E_{\gamma \max} = 23.5$ and 27.5 MeV evidently results from the strongest transitions, $1f_{5/2} \rightarrow 1g_{7/2}$ and $1f_{7/2} \rightarrow 1g_{9/2}$, for which $(b/a)_{\text{theor}} = 0.83$.

The author is deeply indebted to R. D. Rozhdestvenskaya and to N. A. Ponomareva for scanning the plates and assisting with the numerical calculations, to R. A. Latypova and V. P. Fomina, who set up the program for treating the experimental data and for calculating geometric corrections, and to the synchrotron crew.

¹P. R. Byerly and W. E. Stephens, Phys. Rev. **83**, 54 (1951).

²M. E. Toms and W. E. Stephens, Phys. Rev. **95**, 1209 (1954).

³W. A. Butler and G. M. Almy, Phys. Rev. **91**, 58 (1953).

⁴A. K. Mann and J. Halpern, Phys. Rev. **82**, 733 (1951).

⁵R. M. Osokina and B. S. Ratner, JETP **32**, 20 (1957), Soviet Phys. JETP **5**, 1 (1957).

⁶Lejin, Osokina, and Ratner, Nuovo cimento **3**, Suppleto 105 (1956).

⁷Lin'kova, Osokina, Ratner, Amirov, and Akindinov, JETP **38**, 780 (1960), Soviet Phys. JETP **11**, 566 (1960).

⁸J. Rotblat, Nature **167**, 550 (1950).

⁹J. Halpern and A. K. Mann, Phys. Rev. **83**, 370 (1951).

¹⁰L. Katz and B. G. Chidley, Yadernye reaktsii pri malykh i srednykh energiakh, Trudy Vsesoyuznoi konferentsii (Nuclear Reactions at Low and Intermediate Energies, Trans. All-Union Conference), November, 1957.

¹¹R. Nathans and J. Halpern, Phys. Rev. **93**, 437 (1954).

¹²Montalbetti, Katz, and Goldemberg, Phys. Rev. **91**, 659 (1953).

¹³D. L. Allan, Nuclear Phys. **24**, 274 (1961).

¹⁴Geller, Halpern, and Muirhead, Phys. Rev. **118**, 1302 (1960); Chidley, Katz, and Kowalski, Can. J. Phys. **36**, 407 (1958).

¹⁵Strominger, Hollander, and Seaborg, Revs. Modern Phys. **30**, 585 (1958).

¹⁶A. G. W. Cameron, Report AECL, CRP-690, Chalk River, Ontario, 1957.

¹⁷A. G. W. Cameron, Can. J. Phys. **36**, 1040 (1958).

¹⁸J. M. Blatt and V. F. Weisskopf, Theoretical Nuclear Physics, John Wiley and Sons, New York, 1952.

¹⁹M. M. Shapiro, Phys. Rev. **90**, 171 (1953).

²⁰J. A. Evans, Proc. Phys. Soc. (London) **73**, 33 (1959).

²¹E. D. Courant, Phys. Rev. **82**, 703 (1951).

²²D. H. Wilkinson, Physica **22**, 1039 (1956).

Translated by I. Emin